Available online at www.sciencedirect.com
ScienceDirect
Bioorganic & Medicinal Chemistry 16 (2008) 2093–2102
Bioorganic & Medicinal Chemistry

Targeting the inverted CCAAT Box-2 of the topoisomerase IIα gene: DNA sequence selective recognition by a polyamide–intercalator as a staggered dimer

Hilary Mackay,[a,b] Toni Brown,[a,b] Jim S. Sexton,[a] Minal Kotecha,[d] Binh Nguyen,[c] W. David Wilson,[c] Jerome Kluza,[d] Boris Savic,[d] Caroline O'Hare,[d] Daniel Hochhauser,[d] Moses Lee[a,b,*] and John A. Hartley[d]

[a]*Department of Chemistry, Furman University, Greenville, SC 29613, USA*
[b]*Department of Chemistry, Hope College, Holland, MI 49433, USA*
[c]*Department of Chemistry, Georgia State University, Atlanta, GA 30303, USA*
[d]*Cancer Research UK Drug-DNA Interactions Group, Department of Oncology, University College London, London W1W 7BS, UK*

Received 20 June 2007; revised 13 October 2007; accepted 17 October 2007
Available online 22 October 2007

Abstract—The synthesis and DNA binding characteristics of a polyamide–intercalator conjugate, designed to inhibit NF-Y binding to the ICB-2 site of the topoisomerase IIα promoter and up-regulate the expression of the enzyme in confluent cells, are reported. Thermal denaturation and CD titration studies demonstrated binding to the cognate sequence (5′-AAGCTA-3′). Formation of ligand-induced CD bands at ~330 nm provided indication that the molecule interacts selectively in the minor groove of DNA. Intercalation was evidenced by a fivefold increase in emission of the intercalator moiety upon binding to the ICB-2 hairpin oligonucleotide. An increase in viscosity of a solution of calf-thymus DNA on addition of the conjugate provided further evidence. The binding affinity of the conjugate was ascertained using SPR (5.6×10^6 M^{-1}), which according to a gel shift assay was capable of inhibiting the binding of NF-Y at a concentration of 50 μM. DNaseI footprinting, using the topoIIα promoter sequence, highlighted the specificity of the conjugate for the cognate site (5′-AAGCTA-3′). Finally, through Western blot analysis, confluent murine NIH 3T3 cells treated with conjugate were found to have enhanced expression of topoIIα. These results suggest that the conjugate can enter the nucleus, bind to its target site, presumably as a stacked dimer, and up-regulate the expression of topoIIα by blocking the binding of NF-Y.

1. Introduction

The synthesis of polyamides capable of controlling gene expression has become a field of intense research. Based on the pairing rules for specific base recognition in the minor groove, polyamide analogs of distamycin A can be designed to target any DNA sequence.[1–3] Many researchers have shown the efficacy of such ligands to inhibit a number of transcription factors in vitro.[4] Within the authors' laboratory, polyamides have been designed to specifically target the inverted CCAAT Box-2 (ICB-2) on the topoisomerase IIα (topoIIα) promoter.[5–7] At confluence nuclear factor-Y (NF-Y) binds to this site causing down-regulation of topoIIα expression, resulting in the reduced efficacy of anti-cancer therapeutics which target this enzyme.[8–10] For example, hairpin polyamide **1** (Fig. 1) was found to bind to 5′-TTGGT-3′, embedded within the 3′-flanking region of the ICB-2 site (Fig. 2a).[5] Further studies demonstrated inhibition of NF-Y and up-regulation of topoIIα-induced strand breaks by etoposide in confluent cells.[11] However, **1** was also found to bind to ICB sites 1 and 3 within the topoIIα promoter. Additionally, the favorable aqueous solubility of **1** was somewhat unusual since the majority of hairpin polyamide molecules often exhibit poor solubility and are generally taken up poorly by cells, especially into the nucleus.[12] Hence, an alternative polyamide motif to target ICB-2 was sought.

Further work resulted in the design of triamide **2** (Fig. 1) to investigate the viability of using simple, monomeric

Keywords: Polyamides; Naphthalimide; ICB-2; Topoisomerase IIα.
* Corresponding author. Tel.: +1 616 395 7190; fax: +1 616 395 7923; e-mail: lee@hope.edu

0968-0896/$ - see front matter © 2007 Elsevier Ltd. All rights reserved.
doi:10.1016/j.bmc.2007.10.059

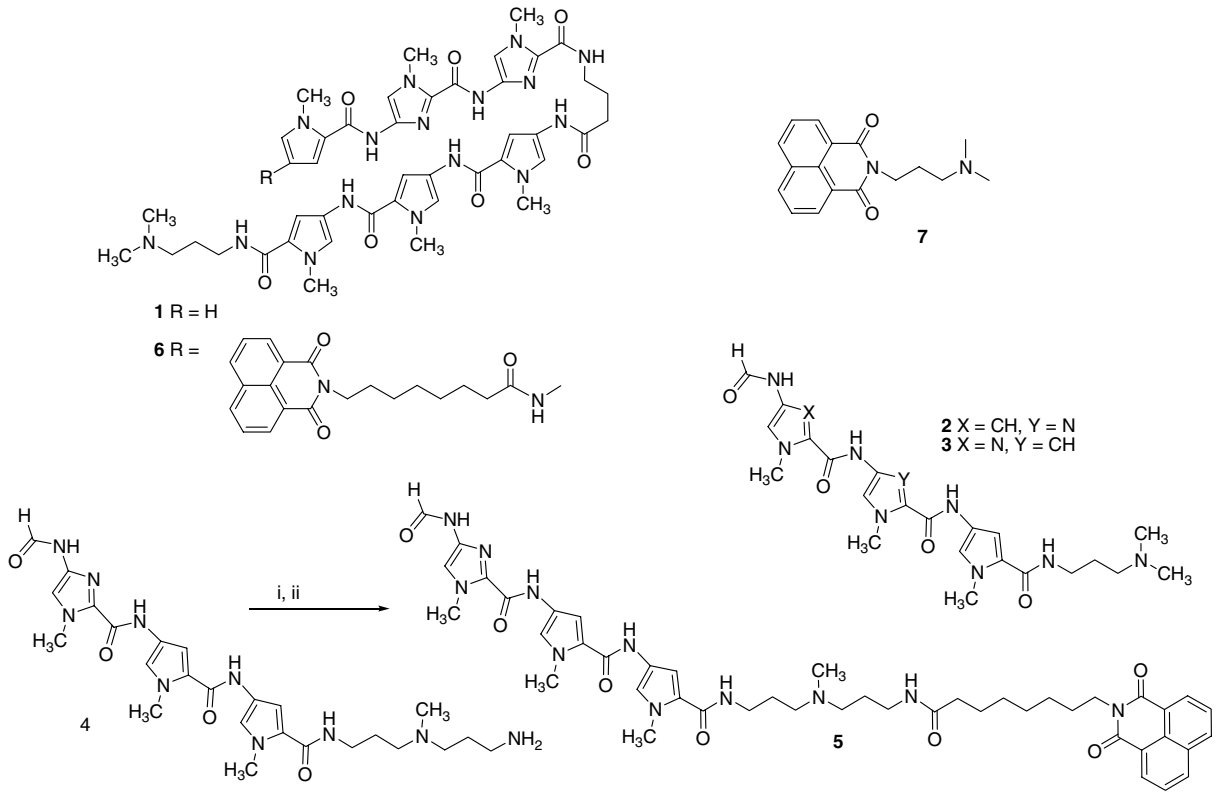

Figure 1. Structures of hairpin polyamides **1a** and **6**, monomer triamides **2** and **3**, polyamide **4** with the extended amine tail, and polyamide–naphthalimide **5**. (i) Naphthalimide caprylic acid, $SOCl_2$, CH_2Cl_2, 25 min, rt; (ii) CH_2Cl_2, THF, TEA, 0 °C–rt, 6 days.

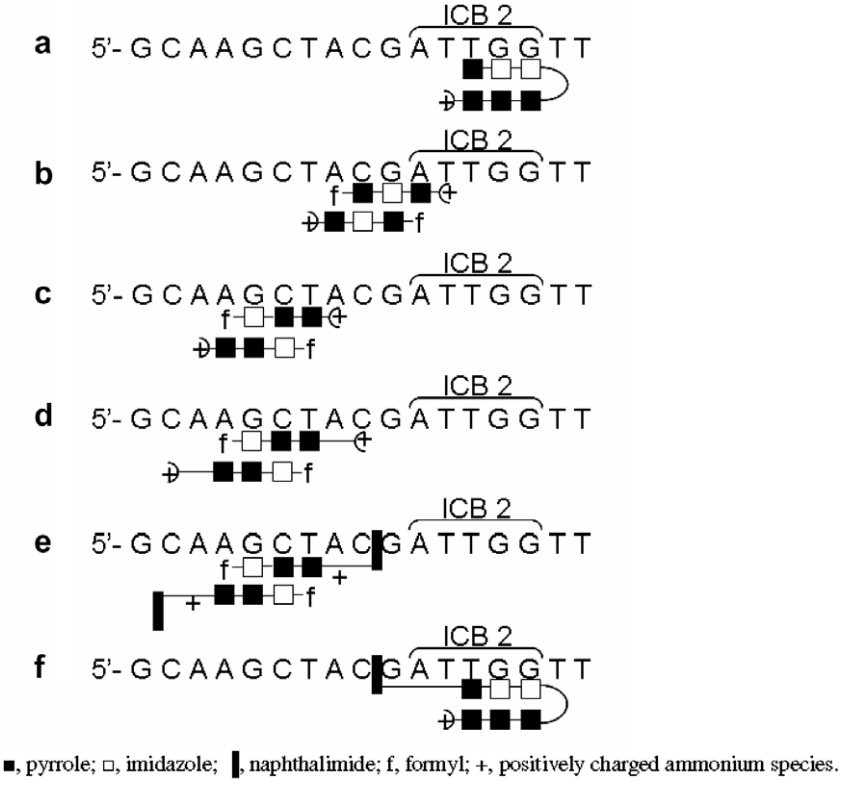

Figure 2. Schematic of compounds **1**–**6** (a–f, respectively) binding to the ICB-2 gene promoter at their appropriate sites.

polyamides, which interact with DNA as dimers, to elicit a biological response.[7] Polyamide **2** was shown, by gel shift assays, to inhibit nuclear factor-Y (NF-Y) by binding to the target sequence 5′-TACGAT-3′, which partially covers the ICB-2 site and its 5′ flank (Fig. 2b).[7] However, DNaseI footprinting and biosensor

surface plasmon resonance (SPR) techniques determined the binding affinity to be low ($K_{eq} = 2 \times 10^5\ M^{-1}$).[13] This could be explained by following the 'core rules' determined previously by the authors' laboratory, whereby the binding affinity of a triamide is dependent on the heterocyclic order at its center: –ImPy–>–PyPy–>>–PyIm– ~ –ImIm–.[13] Triamide **3** (Fig. 1) with a strong –ImPy– core was thus designed to target 5′-AAGCTA-3′ flanking the 5′-ICB-2 site (Fig. 2c). Results from SPR studies demonstrated that **3** bound selectively to a cognate sequence 5′-ATGCAT-3′, which is related to aforementioned target site, with a binding affinity 100-fold greater than **2**.[13] However, inhibition of NF-Y binding was not observed for this molecule at concentrations as high as 50 μM (unpublished data). Based on a recent report by the Dervan group, it was hypothesized that **3** bound too far from the transcription site (three base pairs from 5′ flank) to sufficiently distort the double helix.[14] It was reported that the inhibitor must bind within at least two base pairs of the transcription site to distort the topology such that the native protein cannot bind.[14]

The current report describes a polyamide–naphthalimide conjugate designed to address this issue. Building on triamide **3**, the C-terminus was extended using an *N*′*N*′-bis-(3-aminopropyl)-*N*-methylamine moiety. The authors' laboratory has previously demonstrated that triamides incorporating this side chain bind with high affinity to their cognate DNA sequences.[15] Introduction of this moiety to **3** should yield a ligand (**4**) (Fig. 1) capable of binding selectively, and with high affinity, to the target (5′-AAGCTA-3′) and another cognate (5′-ATGCAT-3′) sites. Moreover, compound **4** also provides an amino functionality that can be derivatized, thereby extending the length of the polyamide, placing the molecule within sufficient range of the ICB-2 site (Fig. 2d). It was decided to derivatize with an intercalating naphthalimide moiety[16] which exhibits a preference for intercalation between G·C base pairs. Introduction of this group to the C-terminus of **4** produces conjugate **5**, and that places the naphthalimide in the ideal position for intercalation between the 5′-C·G base couplet on the ICB-2 flank (Fig. 2e).[17] The author's laboratory has previously employed this strategy in the synthesis of a hairpin polyamide–naphthalimide (**6**) targeted toward ICB-2 (Fig. 2f).[6a] It was determined that the naphthalimide moiety was a suitable intercalator since it did not interfere with the sequence selectivity of the parent hairpin polyamide for its cognate DNA. Additionally, the overall binding affinity of the hybrid **6** was greater than that of a control species without the intercalator. This was attributed to a 100-fold reduced dissociation rate as determined by SPR.[6a] Moreover, a pyrrolobenzodiazepine–naphthalimide conjugate was recently reported that showed the intercalator moiety to DNA binding and cytotoxicity.[6b] However, as is common with most hairpin motifs, this hybrid was found to have complications relating to dissolution and aggregation in solution. The current hybrid **5** has a molecular mass of almost half that of hairpin hybrid **6**, which is expected to alleviate such physiochemical problems. In addition to improved binding affinity, use of an intercalator in the present study will force the side chain to stretch along the DNA and increase the binding site size to 10 base pairs, well within range of the ICB-2 site. Accordingly, the synthesis and DNA binding characteristics of conjugate **5**, in addition to its in vitro effects on NF-Y binding and topoIIα regulation, are described.

2. Results and discussion

2.1. Synthesis

The syntheses of **3** and **4** have been published previously by the authors' laboratory.[15,18] Conjugate **5** was prepared from **4** via a standard acid chloride coupling with naphthalimidoyl-caprylic acid (Fig. 1).[6]

2.2. Thermal denaturation

Thermal denaturation analyses were carried out to determine the selectivity of the polyamides for their cognate sequences. The data in Table 1 show that **5** demonstrates good affinity to its cognate sequence (AAGCTA) with a ΔT_m of 8.4 °C. This is reduced in comparison to **4** which yielded a striking ΔT_m of >22 °C. This reduction could be a result of the loss of a positive charge from the terminal amine upon introduction of the naphthalimide moiety, and it could also explain the lower ΔT_m value of 5.1°C for monocation **3**. Compound **5** also binds to the non-cognate A·T rich sequence, but with >2-fold less affinity. This is true also for **4**, suggesting that the introduction of the intercalator does not affect selectivity.

2.3. Circular dichroism (CD)

CD studies were performed to provide evidence for DNA minor groove binding. The spectra in Figure 3 show strong, minor groove binding of both **4** and **5** to the cognate sequence (AAGCTA) as indicated by the induced band at ~330 nm.[13,19] However, the binding of **5** is slightly reduced in comparison to **4**. Concurrent with the denaturation studies, both compounds also demonstrate binding to their non-cognate A·T rich sequences, yet to a lesser extent. These results ascertain that the intercalator does not alter the selectivity of the polyamide moiety.

Table 1. ΔT_m values (°C) of **3**, **4**, and **5** with cognate and non-cognate DNA hairpins

	ATGCAT	AAATTT 11 bp	AAATTT 10 bp	AAGCTA	AAATTT 12 bp
3	11.0	3.5		5.1	
4			10.0	>22.0	
5				8.4	3.8

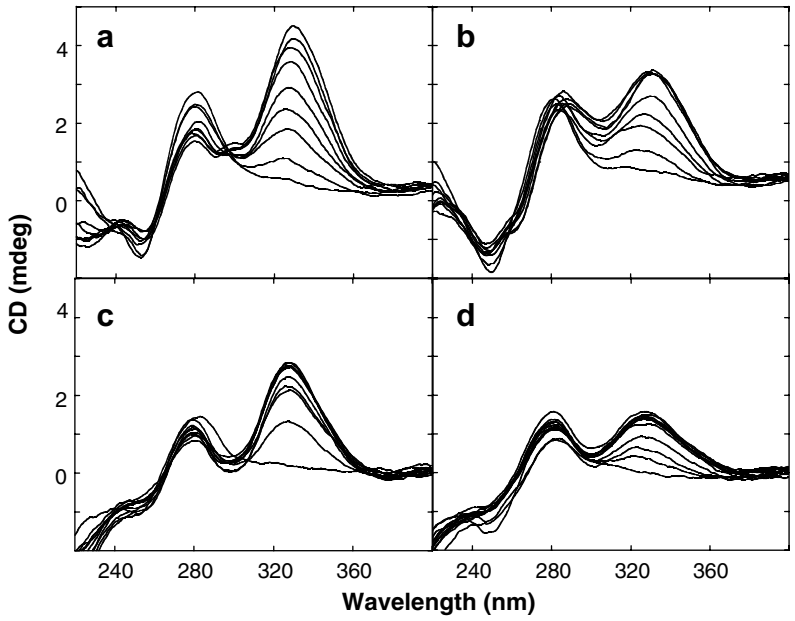

Figure 3. Circular dichroism spectra of **4** with cognate AAGCTA (a) and non-cognate AAATTT 10 bp (b), and compound **5** with cognate AAGCTA (c) and non-cognate AAATTT 12 bp (d). Experiments used a 9 μM DNA solution in phosphate buffer to which **4** or **5** was titrated in 0.5 or 1 molar equivalents until past the point of saturation.

2.4. Emission studies

Intercalating agents, such as ethidium bromide, bind to DNA with a concomitant increase in emission intensity (>25-fold).[20] Evidence for intercalation of **5** is provided by the emission spectra in Figure 4. It can be observed that the area under the emission peak at ~390 nm increases in magnitude fivefold with each titration of DNA into a sample of **5**, up to a mole ratio of 10:1 ligand:DNA. This result compares favorably with evidence of intercalation by compound **6**, as well as the intercalator **7** alone, which gave a 4.5-fold increase in emission.[6] Thus, it can be inferred that binding of **5** to DNA includes an intercalative binding mode.

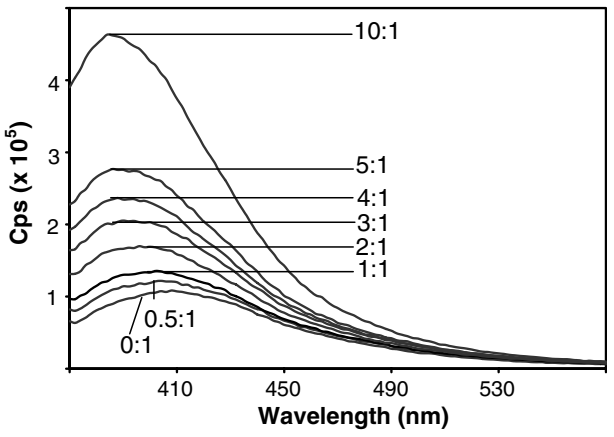

Figure 4. Emission spectrum of **5** with its cognate DNA sequence (AAGCTA). Compound **5** was titrated into a solution of DNA (0.3 mM, 10 mM phosphate buffer) in 0.5–1 molar aliquots until a concentration of 10 molar equivalents was reached.

3. Viscosity

Intercalation enhances the viscosity of a solution of DNA due to a lengthening of the helix and an associated decrease in the average mass per unit length DNA.[21] Further evidence of intercalation of **5** was provided using viscosity measurements with calf-thymus (CT) DNA (Fig. 5a). Upon titration of **5** into CT DNA, the viscosity of the DNA solution increased, indicating intercalation. In comparison to the naphthalimide moiety alone **7** (Fig. 5b), compound **5** increased viscosity to a lesser extent. This is attributed to **5** selectively binding within the minor groove of CT DNA as dictated by the polyamide moiety. The number of intercalation sites is thus reduced in comparison to naphthalimide alone. It can therefore be inferred that, like the intercalator **6** alone, **5** associates with the DNA via intercalation or partial intercalation after polyamide minor groove binding, an observation that cannot be determined through emission studies.

3.1. Surface plasmon resonance

SPR analyses provide information from which the binding constant of **5** to its cognate sequence can be calculated. Analysis of the steady-state binding data given in Figures 6a and 6b (Table 2a) of **5** to the cognate sequence (5′-biotin-AAGCTA) yielded a binding affinity comparable to that of the parent polyamide (**3**) ($K = 5.6 \times 10^6$ and 5.5×10^6 M^{-1}, respectively), which is consistent with the ΔT_m values for both compounds. It had been anticipated that the intercalating moiety would enhance the binding affinity of the polyamide alone. Although this result was not obtained, it can at least be ascertained that addition of the intercalator is not detrimental to binding affinity. However, in corroboration with prior biophysical analyses, **5** is >10-fold more selective for the cognate

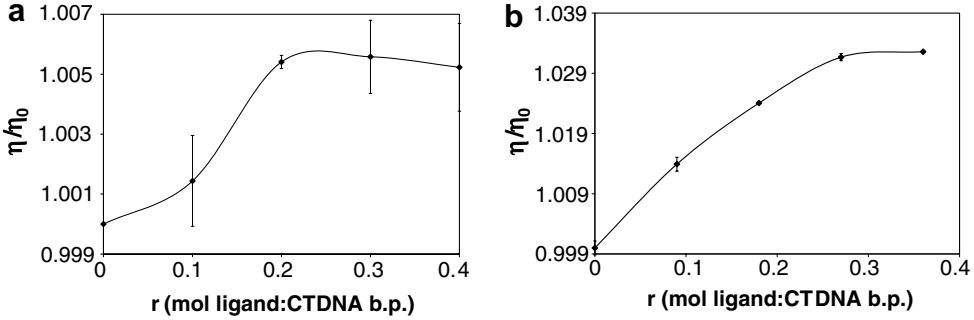

Figure 5. Viscosity studies of increasing concentration of **5** (a) and **7** (b) with CT DNA (0.3 mM, 10 mM phosphate buffer). Experiments were carried out at 27 °C (±0.05 °C) and compounds **5** and **7** added until past the point of saturation; η/η_0 = average flow time of DNA:ligand solution over the average flow time of DNA solution.

Table 2a. The steady-state binding affinities ($K = (K_1 \times K_2)^{1/2}$ M^{-1}) for **3** and **5** to three DNA hairpins

Affinity (M^{-1})	5′-Biotin-ACGCGT	5′-Biotin-AAGCTT	5′-Biotin-AAATTT
3	9.5×10^4 (2.9×10^4, 3.0×10^5)	5.5×10^6 (4.5×10^5, 6.6×10^7)	4.7×10^5 (1.2×10^6, 1.8×10^5)[a]
5	2.8×10^5 (1.3×10^5, 5.7×10^5)	5.6×10^6 (1.4×10^5, 4.4×10^8)	1.5×10^5 (1.2×10^6, 1.8×10^5)

[a] The figures given inside the parentheses are K_1 and K_2, respectively.

sequence over the two non-cognate sequences (5′-biotin-ACGCGT and 5′-biotin-AAATTT). Additionally, the expected stoichiometry of 2:1 (ligand:DNA) was determined, providing evidence of the anticipated staggered-dimer binding motif. The data also suggest cooperative binding of **5** to the cognate sequence as anticipated ($K_2 > K_1$). The binding affinities obtained via kinetic analyses (Table 2b) are comparable to those obtained via steady-state calculations. However, the association and dissociation rates of **5** are 10-fold faster than those of **3**. Therefore, addition of an intercalator facilitates the binding kinetics without changing the binding affinity. This was an unexpected result: the intercalator was thought to improve the overall binding affinity by slowing the dissociation rate as was previously observed with hairpin-naphthalimide **6**.[6a] This may suggest that the binding of the naphthalimide is only pseudo-intercalative, whereby, the chromophore is only partially inserted between the tilted base pairs. This observation is not uncommon of aromatic compounds. For example, berberine, an aromatic alkaloid, is known to bind DNA in a partial intercalation mechanism.[6c]

Due to possible mass transfer issues that can influence the interaction kinetics in SPR experiments, independent dissociation kinetics from CD experiments were conducted with the same biotin labeled hairpins. The results were consistent with the SPR data: **5** dissociates seven times faster than **3** ($t_{1/2}$**5**:DNA complex ~108 s compared to **3**:DNA ~770 s, Fig. 6c). The results from SPR and CD studies suggest that the intercalating moiety must interact with the DNA with fast kinetics; hence, the effects on the dissociation rate constant were minimal. This could also explain the fact that similar footprints were observed for compounds **3** and **5**, despite the extended length of **5**.

3.2. DNaseI footprinting

To further study the binding affinity and selectivity of **5**, DNaseI footprinting was carried out using a 479 bp 5′-[32]P-radiolabeled fragment containing the topoisomerase IIα promoter. At a concentration of 3 μM **5**, a clear footprint at 5′-AAGCTA-3′, located at the ICB2 5′-flank, is observed (Fig. 7), corroborating prior biophysical analyses. Polyamide **3** shows stronger binding with a footprint beginning to appear at 0.3 μM, however, a footprint at the non-cognate site 5′-A(537)GCGAGTC A(545)-3′ can be observed. This indicates that polyamide sequence selectivity is enhanced by the naphthalimide moiety (presumably via its preference for C·G), and that a groove binding mode is required for overall conjugate binding. Neither compound showed a footprint at ICB3 sites (442–446), indicating the selectivity for the 5′-flanking 5′-AAGCTA-3′ site of ICB2. It is surprising that no enhanced DNaseI cleavage is observed at

Table 2b. Comparison of kinetic data obtained for **3** and **5** with cognate DNA (5′-AAGCTA) using Biacore and CD techniques (k_a [M^{-1} s^{-1}]; k_d [s^{-1}]; k_a/k_d [M^{-1}])

	Biacore kinetics			CD kinetics	
	k_a	K_d	k_a/k_d	k_a	k_d
3	1.8×10^4	3.2×10^3	5.5×10^6	5.0×10^3	9.0×10^{-4}[a] (1.6×10^{-3})[b]
5	1.7×10^5	2.2×10^{-2}	7.7×10^6	4.9×10^4	6.4×10^{-3}[a] (5.0×10^{-3})[b]

[a] The average dissociation rate constants obtained from the half-life of the CD dissociation curve.
[b] The average dissociation rate constants obtained from exponential fit of the CD dissociation curve.

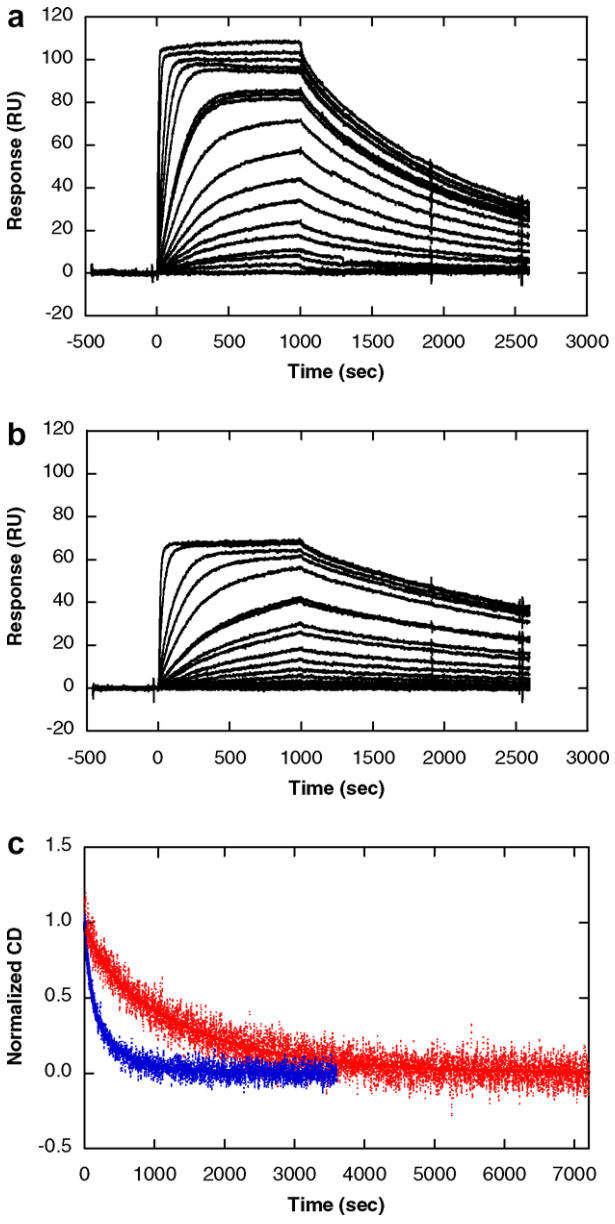

Figure 6. SPR sensorgrams of **5** (a) and **3** (b) with 5′-biotin-AAGCTA (concentration of lowest and highest sensorgrams is 0 and 4 μM, respectively). (c) The normalized SDS-induced CD plot of **3** and **5** ($CD_{normalized} = CD/(A_0 + A_1 + A_2)$).

the site of naphthalimide binding, as would be expected in the case of true intercalation. In corroboration with the SPR results, this is again suggestive of a partial intercalative mode. However, at a higher concentration of compound **5** a few enhanced cleavage sites can be observed, suggesting that the threshold of sequence selectivity is less than 10 μM.

3.3. Gel shift studies

Electrophoretic mobility shift assays (EMSA) can provide direct evidence for the ability of small molecules to inhibit the binding of transcription factors to their DNA sites.[10] EMSA studies for the binding of **5** to 5′-[32]P radiolabeled ICB2-containing DNA fragments were thus conducted. At a concentration of 50 μM, **5** completely inhibited protein binding, present in nuclear extracts of confluent cells, to the ICB-2 oligonucleotide (Fig. 8a). In contrast, **3** does not show inhibition (Fig. 8b) at this concentration, indicating that the addition of the naphthalimide and linker has extended the length sufficiently to interfere with NF-Y binding.[14]

3.4. Western blotting

Western blot analyses with NIH 3T3 cells, cultured to confluence, were performed to demonstrate the ability of monomeric polyamides to enter the nucleus and affect gene expression. Confluent NIH 3T3 cells were incubated with compound **5** and analyses performed after 6 and 24 h. The results (Fig. 9) confirm that topoIIα protein expression in confluent cells was reduced as compared to exponentially growing cells.[8] Compound **5** was found to induce topoIIα protein expression after 24 h of exposure. This is most clearly observed at a drug concentration of 10 μM, but even at a concentration of 1 μM, the band can be discerned.

4. Conclusion

Whilst hairpin polyamides have been shown to possess remarkable sequence selectivity, their poor aqueous solubility and large molecular mass limit their biological application.[12] The current report demonstrates that simple, monomer polyamides, which bind in a staggered-dimer motif, can be designed to inhibit transcription factors in cells grown in culture. Thermal denaturation, CD, and DNaseI footprinting demonstrated that polyamide–intercalator hybrid **5** bound selectively to the desired cognate DNA sequence (3′-AAGCTA-5′). SPR determined the binding affinity to the cognate to be reasonably strong and comparable to that of the parent molecule (**3**). It was shown that conjugate **5** bound to DNA via both minor groove binding and pseudo-intercalation as intended: CD indicated the presence of a DNA minor groove binding mode, whilst fluorescence and viscosity experiments provided evidence for partial intercalation. Similarities between the SPR derived binding constants of **3** and **5**, and the absence of enhanced DNaseI cleavage at the binding site further suggest that intercalation is only partial. Gel shift studies demonstrated that **5** inhibited NF-Y binding to the ICB-2 site and Western blot analyses confirmed up-regulation of topoIIα expression in confluent NIH 3T3 murine fibroblast cells. These results indicate that monomeric polyamides can overcome the hurdle of nuclear uptake, and thus have the potential to be used as gene control agents. Studies are ongoing to develop modified polyamides with increased binding affinity.

5. Experimental

5.1. Synthesis

5.1.1. Synthesis of 4. Procedure adapted from Ref. 15 to yield **4** as a white solid (40 mg, 100%), mp 110–123 °C:

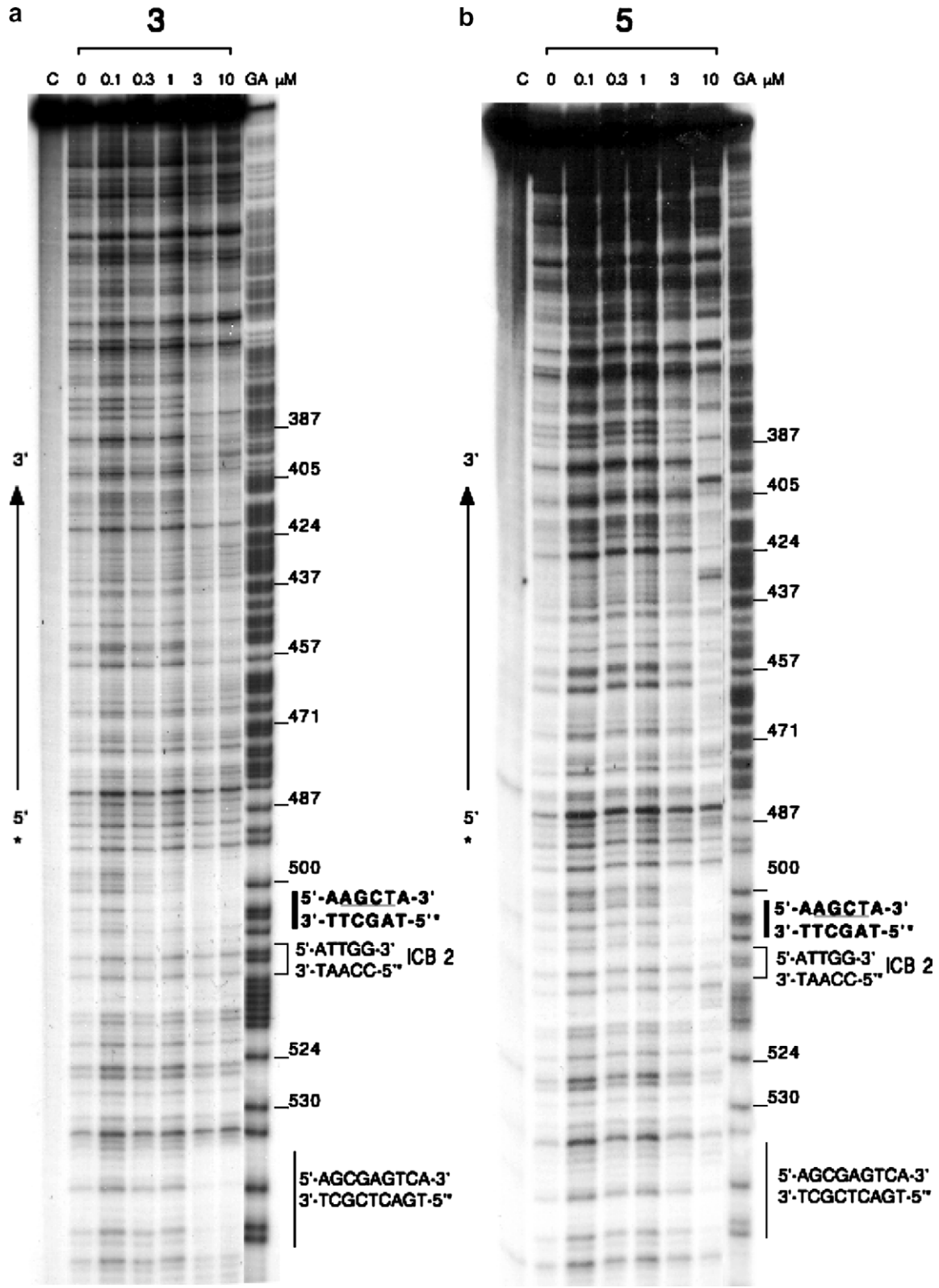

Figure 7. DNaseI footprinting of **3** (a) and **5** (b). Lane 1 contains a blank control, lanes 2–7 contain compound in increasing concentration (0, 0.1, 0.3, 1, 3, and 10 μM), and lane 8 is the G-A sequencing lane. Brackets indicate ICB2 sites and solid lines indicate the target footprinting sites.

^{1}H NMR (CD_3OD) 8.25 (s, 1H); 7.42 (s, 1H); 7.28 (d, 1H, J = 1.5 Hz); 7.22 (d, 1H, J = 2 Hz); 6.98 (d, 1H, J = 1.5 Hz); 6.93 (d, 1H, J = 2 Hz); 4.04 (s, 3H); 3.92 (s, 3H); 3.89 (s, 3H); 3.42 (t, 2H, J = 6.5 Hz); 3.26 (t, 2H, J = 7.5 Hz); 3.21 (m, 2H); 3.08 (t, J = 6.5 Hz, 2H); 2.90 (s, 3H); 2.08 (m, 4H); IR (neat) ν 3367, 2954, 1645, 1555, 1435, 1405, 1267, 1211, 1123, 1016 cm^{-1}; MS (ES+) m/z (rel intensity) 541 ([M+H], 60%); HRMS

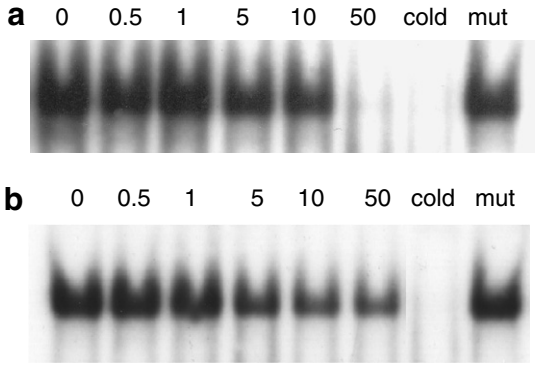

Figure 8. EMSA studies of **5** (a) and **3** (b) using oligonucleotides containing the ICB2 sequence. Lanes 1–6 contain **5** or **3** in increasing concentration (0–50 μM), lane 7 contains unlabeled oligonucleotide and lane 8 contains mutated oligonucleotide.

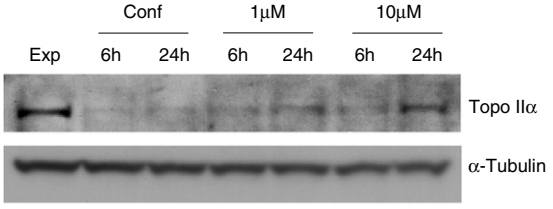

Figure 9. Western blot analysis of **5** in NIH 3T3 cells. Lane 1 contains untreated exponentially growing cells, lanes 2 and 3 contain cells maintained at confluence for 6 and 24 h, lanes 4 and 5 contain **5** at concentration of 1 μM and lanes 6 and 7 contain **5** at a concentration of 10 μM. Western blot analysis was carried out on samples after +6 and +24 h. Tubulin is shown as a loading control.

m/*z* calcd for $C_{25}H_{36}N_{10}O_4$ $[M+H]^+$ 541.2999; found 541.3000.

5.1.2. Synthesis of 5. 8-(1,3-Dioxo-1H-benzo[de]isoquinolin-2(3H)-yl)octanoic acid[6] (38.3 mg, 0.113 mmol) was refluxed in $SOCl_2$ (0.5 mL) and CH_2Cl_2 for 25 min. The solution was concentrated via vacuum aspiration, and the resulting yellow solid coevaporated with CH_2Cl_2 (2× 3 mL). This yellow solid was then redissolved in CH_2Cl_2 (~5 mL) and added dropwise to a suspension of **4** in THF (~5 mL) and TEA (0.011 mL, 0.0814 mmol) over ice. After stirring at RT for 6 days, the reaction mixture was washed with satd aq $NaHCO_3$ and then extracted with CH_2Cl_2 (20× 2 mL) and EtOAc (20× 1 mL). The combined organic layers were dried (Na_2SO_4) and concentrated under reduced pressure. The product was purified via column chromatography over silica ($CHCl_3$/MeOH gradient) to yield a beige solid (8.5 mg, 30%), mp 102–105 °C; ^1H NMR ($CDCl_3$) 8.96 (s, 1H); 8.79 (s, 1H); 8.59 (d, 2H, J = 8.0 Hz); 8.35 (s, 1H); 8.21 (d, 2H, J = 8.0 Hz); 7.74 (t, 2H, J = 8.0 Hz); 7.39 (s, 1H); 7.30 (s, 1H); 7.24 (s, 1H); 6.83 (s, 1H); 6.65 (s, 1H); 4.13 (t, 2H, J = 7.0 Hz); 4.01 (s, 3H); 3.93 (s, 3H); 3.90 (s, 3H); 3.75 (br t, 2H); 3.44 (m, 2H); 3.32 (quin br, 2H); 2.55 (m, 4H); 2.33 (s, 3H); 2.19 (t, 2H, J = 7.0 Hz); 1.8 (m br, 4H); 1.69 (m, 2H); 1.37 (m, 6H). IR (neat) ν 3352 (br), 2928, 2856, 2361, 1654, 1540, 1437, 1237 cm^{-1}; MS (ES+) *m*/*z* (rel intensity) 862 ([M+H], 100%); HRMS *m*/*z* calcd for $C_{45}H_{55}N_{11}O_7$ $[M+H]^+$ 862.4364; found 862.4368.

5.2. Thermal denaturation

The synthetic DNA hairpins used in these studies were obtained from Operon (Huntsville, AL): **ATGCAT**, CGGAATGCATTCTCTAATGCATTCCG; **AAGC TA**, GGCAAGCTACGACTCT-TCGTAGCTTGCC; **A AATTT** 11 bp, GGCGAAATTTCC-TCTGAAATTT CGCC; **AAATTT**10 bp, CGAAATTTCCCTCTGGAA ATTTCG; **A-AATTT**12 bp, GCGAAATTTCGGCTC TC-CGAAATTTCGC. Data were obtained using a Cary Bio 100 spectrophotometer and cells with a 10 mm pathlength. Experiments were performed in $PO_4$0 (10 mM sodium phosphate, 1 mM EDTA, pH 6.2) with 1 μM oligonucleotide and 3 μM ligand. Oligonucleotide samples were reannealed prior to denaturation studies by heating at 70 °C for 1 min and then allowing to cool to RT. The temperature was programmed to ramp from 25 to 95 °C at a rate of 0.5 °C/min recording the Abs_{260} every 0.5 °C. The data were analyzed using KaleidaGraph (Synergy Software, Reading PA) and the T_m values determined as the maximum of the first derivative.

5.3. Circular dichroism

CD studies were performed on a JASCO J-710 spectrophotometer using the oligonucleotides detailed above. Experiments were conducted at ambient temperature in a 1 mm pathlength cuvette. The initial DNA concentration was 9 μM in $PO_4$5 (10 mM phosphate, 50 mM Na^+, and 1 mM EDTA, pH 6.2) and a solution of ligand was titrated in aliquots of 0.5 or 1 molar equivalents past the point of saturation.

5.4. Emission studies

Steady-state emission spectral measurements were recorded using a SPEX Fluorolog 2 fluorimeter employing a red sensitive Hamamatsu R928 photomultiplier tube. Emission was detected via a J-Y Optics H10V monochromator and a Hamamatsu R928 photomultiplier tube. The slit width for the experiment was set at 1 mm for excitation and 4 mm for collection. In a 0.2 mm cell, a solution of 0.1 μM ligand in $PO_4$20 (10 mM phosphate, 200 mM Na^+, and 1 mM EDTA, pH 6.2) was excited at 306 nm. Calf-thymus (CT) DNA was diluted in $PO_4$20 and titrated in aliquots of 0.5 molar equivalents until a 10:1 DNA:ligand ratio was reached. Emission data were collected over the range 375–560 nm in one continuous scan.

5.5. Viscosity

CT DNA (1100 μL, 0.3 mM, $PO_4$20) was placed in the sample reservoir of a CT-500 series II viscometer and a stop watch used to record the length of time taken for DNA to flow through the measurement reservoir (±0.1 s). Experiments were carried out at 27 °C (±0.05 °C) and time measurements taken in triplicate. Polyamide (8 μL, 3.5 mM) was then titrated into the

DNA solution and times again recorded in triplicate. The mole ligand:DNA was then plotted against the average flow time of DNA:ligand solution over the average flow time of DNA solution (η/η_0).

5.6. SPR

5′-Biotin labeled DNA hairpins were purchased from Integrated DNA technologies, Inc. (Coralville, IA) with HPLC purification: **ACGCGT**, 5′-biotin-CCGACGCG TCGGCTC-TCCGACGCGTCGG; **AAGCTA**, 5′-biotin-GGCAAGCTACGACTCTTCGTAGCTT-GCC; **AAATTTT**, 5′-biotin-CGAAATTTCCTCTGAAATTTC G. Experiments were conducted on a BIACORE 2000 (Biacore, AB) instrument in degassed MES buffer (10 mM, 200 mM Na^+, 1 mM EDTA, 5×10^{-5} v/v P20-Biacore surfactant (10%), pH 6.25) at 25 °C. DNA hairpins were immobilized on a streptavidin-derivatized chip (SA Chip, Biacore) by manual injection of 25 nM DNA solution, with a flow rate of 1 μL/min until the 400–450 response units (RU) were reached. Flow cell 1 was left blank whilst cells 2–4 were immobilized with three different DNA hairpins. Typically, a series of concentrations of ligand was injected onto the chip at a flow rate of 15 μL/min for a period of 16.7 min, followed by a dissociation period of 25 min. After each cycle, the chip surface was regenerated with a 10 μL injection of NaOH solution (25 mM, 500 mM NaCl). Injection tube rinsing and multiple 1 min buffer injections were then carried out. At low concentrations, where the steady-states were not fully reached, equilibrium responses were obtained from kinetic fits of these sensorgrams. The observed steady-state responses, RU_{obs}, were divided by predicted maximum response per ligand, RU_{max}, and plotted against the free ligand concentrations, L, and fitted with a 2:1 model.

$$r = (RU_{obs}/RU_{max}) = (K_1 \times L + 2 \times K_1 \times K_2 \times L^2)/(L + K_1 \times L + K_1 \times K_2 \times L^2)$$

CD: The sodium dodecyl sulfate (SDS) induced dissociation kinetics of **3** and **5** with the cognate sequence 5′-biotin-AAGCTA were determined as follows; DNA hairpin (3 μM) and ligand (9 μM) were mixed in MES buffer and SDS solution (1% w/v) added to the sample with a mixing time of ~10 s (<3% dilution). The CD change at 327 nm was immediately monitored over a period of 1–2 h at 25 °C in duplicate. The CD baseline was obtained in a similar manner without the DNA. The average value from the baseline CD was subtracted from the complex dissociation CD. The corrected CD change as a function of time was fitted with an exponential decay equation.

$$CD = A_1 \times e^{(-kd2 \times t)} + A_2 \times e^{(-kd2 \times t)} + A_0 \text{(where } k_{d1} \text{ and } k_{d2} \text{ are dissociation rate constants)}$$

5.7. DNaseI footprinting

A radiolabeled probe of 479 bp corresponding to positions −489 through −10 relative to the transcriptional start site of the topoIIα promoter was generated as follows. Four picomole of the antisense oligonucleotide 5′-GTCGGTTAGGAGAGCTCCACTTG-3′ was 5′-end labeled with T4 kinase (Invitrogen, Paisley, UK) using [γ-^{32}P]ATP in a 10 μL reaction, followed by heat inactivation for 20 min at 65 °C. Subsequently, 4 pmol sense oligonucleotide (5′-CTGTCCAGAAAGCCG GCACT CAG-3′), 2 μL of 10 mM dNTPs (Promega, Southampton, UK), 1 U Red Hot DNA Polymerase (Abgene, Epsom, UK), 2 μL of 25 mM $MgCl_2$, and 4.5 μL of 10× reaction buffer IV (Abgene, Epsom, UK) were added (in a final volume of 50 μL) and a PCR was performed consisting of: 3 min at 95 °C and 1 min at 95 °C, 1 min 60 °C and 2 min 72 °C for 35 cycles. The product was purified on a Bio-Gel P-6 column (Bio-Rad, Hemel Hempstead, UK). DNA*se* I footprint reactions were performed with 30 μg nuclear extract in a 50 μL reaction in the same buffer as used for EMSA. After pre-incubation for 30 min at 4 °C approximately 0.1 ng radiolabeled probe was added and the mixture was incubated at room temperature for another 30 min. Subsequently, 1 U RQ1 DNA*se* I (Promega, Southampton, UK) and up to 5 mM $MgCl_2$ and $CaCl_2$ were added. Following exactly 3 min of digestion at room temperature, 1 volume stop mix containing 30 mM K-EDTA, pH 8.0, 200 mM NaCl, and 1% SDS was added and samples were purified by phenol–chloroform treatment and alcohol precipitation. The resulting pellets were dried and re-suspended in loading buffer (95% formamide, 20 mM K-EDTA, pH 8.0, 0.05% BFB, and 0.05% xylene cyanol). The sample was heat denatured for 3 min at 95 °C and separated on a 6% denaturing polyacrylamide gel (Sequagel, National Diagnostics, East Riding, Yorkshire, UK). A 10 bp ladder (Invitrogen, Paisley, UK) labeled with ^{32}P by T4 kinase was used as a molecular weight standard. The dried gels were exposed to Kodak X-Omat-LS film with intensifying screens (Kodak, UK) at −80 °C.

5.8. Electrophoretic mobility shift assay (EMSA)

5′-end labeled oligonucleotide 5′-GGCAAGCTACGAT TGGTTCTTCTGGACG-3′ containing the ICB2 sequence (underlined) was incubated with **5** and **3** (concentrations ranging from 0 to 50 μM) for 2 h prior to incubation with nuclear extracts from cultured confluent NIH 3T3 cells and EMSA as previously described.[11]

5.9. Western blotting

NIH 3T3 cells were either exponentially growing (Exp) or maintained at confluence for 96 h (Conf). Confluent cells were treated with 1 or 10 μM polyamide **5** and Western blot analysis carried out as previously described[11] on samples collected at +6 and +24 h post-treatment. The 1H1C8 rabbit polyclonal topoIIα antibody was used for Western blotting and tubulin used as a loading control.

Acknowledgments

The authors thank NSF (CHE-0550992), Medical Research Council UK (G0000168), and Cancer Research UK (C2259/A3083) for support.

References and notes

1. Dervan, P. B.; Edelson, B. S. *Curr. Opin. Struct. Biol.* **2003**, *13*, 284.
2. Kopka, M. L.; Goodsell, D. S.; Han, G. W.; Chiu, T. K.; Lown, J. W.; Dickerson, R. E. *Structure* **1997**, *5*, 1033.
3. Yang, X.-L.; Hubbard, R. B., IV; Lee, M.; Tao, Z.-F.; Sugiyama, H.; Wang, A. H.-J. *Nucleic Acids Res.* **1999**, *27*, 4183.
4. Melander, C.; Burnett, R.; Gottesfeld, J. M. *J. Biotechnol.* **2004**, *112*, 195.
5. Henry, J. A.; Le, N. M.; Nguyen, B.; Howard, C. M.; Bailey, S. L.; Horick, S. M.; Buchmueller, K. L.; Kotecha, M.; Hochhauser, D.; Hartley, J. A.; Wilson, D. W.; Lee, M. *Biochemistry* **2004**, *43*, 12249.
6. (a) Flores, L. V.; Staples, A. M.; Mackay, H.; Howard, C. M.; Uthe, P. B.; Sexton, J. S., III; Buchmueller, K. L.; Wilson, W. D.; O'Hare, C.; Kluza, J.; Hochhauser, D.; Hartley, J. A.; Lee, M. *ChemBioChem* **2006**, *7*, 1722; (b) Kamal, A.; Reddy, B. S.; Reddy, G. S.; Ramesh, G. *Bioorg. Med. Chem. Lett.* **2002**, *12*, 1933; (c) Yadav, R. C.; Kumar, G. S.; Bhadra, K.; Giri, P.; Sinha, R.; Pal, S.; Maiti, M. *Bioorg. Med. Chem.* **2005**, *13*, 165.
7. Le, N. M.; Sielaff, A. M.; Cooper, A. J.; Mackay, H.; Brown, T.; Kotecha, M.; O'Hare, C.; Hochhauser, D.; Lee, M.; Hartley, J. A. *Bioorg. Med. Chem. Lett.* **2006**, *16*, 6161.
8. Isaacs, R. J.; Harris, A. L.; Hickson, I. D. *J. Biol. Chem.* **1996**, *271*, 16741.
9. Ronchi, A.; Bellorini, M.; Mongelli, N.; Mantovani, R. *Nucleic Acids Res.* **1995**, *23*, 4565.
10. Tolner, B.; Hartley, J. A.; Hochhauser, D. *Mol. Pharmacol.* **2001**, *59*, 699.
11. Hochhauser, D.; Kotecha, M.; O'Hare, C.; Morris, P. J.; Hartley, J. M.; Taherbhai, Z.; Harris, D.; Forni, C.; Mantovani, R.; Lee, M.; Hartley, J. A. Mol. *Cancer Ther.* **2007**, *6*, 346.
12. Belitsky, J. M.; Leslie, S. J.; Arora, P. S.; Beerman, T. A.; Dervan, P. B. *Bioorg. Med. Chem.* **2002**, *10*, 3313.
13. Buchmueller, K. L.; Staples, A. M.; Howard, C. M.; Horick, S. M.; Uthe, P. B.; Le, N. M.; Cox, K. K.; Nguyen, B.; Pacheco, K. A. O.; Wilson, W. D.; Lee, M. *J. Am. Chem. Soc.* **2005**, *127*, 742.
14. Gearhart, M. D.; Dickinson, L.; Ehley, J.; Melander, C.; Dervan, P. B.; Wright, P. E.; Gottesfeld, J. M. *Biochemistry* **2005**, *44*, 4196.
15. Brown, T.; Taherbhai, Z.; Sexton, J.; Sutterfield, A.; Turlington, M.; Jones, J.; Stallings, L.; Stewart, M.; Buchmueller, K.; Mackay, H.; O'Hare, C.; Kluza, J.; Hartley, J.; Nguyen, B.; Wilson, D.; Lee, M. *Bioorg. Med. Chem.* **2007**, *15*, 474.
16. Brana, M. F.; Ramos, A. *Curr. Med. Chem. Anticancer Agents* **2001**, *1*, 237.
17. Feigon, J.; Denny, W. A.; Leupin, W.; Kearns, D. R. *J. Med. Chem.* **1984**, *27*, 450.
18. Lacy, E. R.; Le, N. M.; Price, C. A.; Lee, M.; Wilson, W. D. *J. Am. Chem. Soc.* **2002**, *124*, 2153.
19. Lyng, R.; Rodger, A.; Norden, B. *Biopolymers* **1992**, *32*, 1201.
20. LePecq, J.; Paoletti, C. *J. Mol. Biol.* **1967**, *27*, 87–106.
21. Lerman, L. S. *J. Mol. Biol.* **1961**, *3*, 18–30.